

# Line Structure in the Spectrum of FU Orionis

P. P. Petrov

*Crimean Astrophysical Observatory,  
p/o Nauchny, Crimea 98409, Ukraine*

and

G. H. Herbig

*Institute for Astronomy, University of Hawaii,  
2680 Woodlawn Drive, Honolulu, HI 96822*

## ABSTRACT

New high-resolution spectra of FU Ori, obtained with the HIRES spectrograph at the Keck I telescope in 2003–2006, make it possible to compare the optical line profiles with those predicted by the self-luminous accretion disk model. A dependence of line width on excitation potential and on wavelength, expected for a Keplerian disk, is definitely not present in the optical region, nor is the line duplicity due to velocity splitting. The absorption lines observed in the optical region of FU Ori must originate in or near the central object, and here their profiles are shown to be those expected of a rigidly rotating object. They can be fitted by a rapidly rotating ( $v \sin i = 70 \text{ km s}^{-1}$ ) high-luminosity G-type star having a large dark polar spot, with axis inclined toward the line of sight. Over these years, the radial velocity of FU Ori has remained constant to within  $\pm 0.3 \text{ km s}^{-1}$ , so there is no indication that the star is a spectroscopic binary. These results apply to the optical region ( $\lambda < 8800 \text{ \AA}$ ); more distant, cooler regions of the disk contribute in the infrared.

*Subject headings:* stars: evolution — stars: individual (FU Orionis) — stars: pre-main-sequence — stars: variables: other

## 1. Introduction

FU Ori is the prototype of a small group of pre-main-sequence stars, the so-called FUors. As explained in the Introduction to Herbig et al. (2003), the first members were optically detectable and so could be studied in some detail. They were distinguished by flareups of several magnitudes followed either by near-constancy or slow decline; by broad-lined absorption spectra resembling F- to K-type supergiants in the optical region; by powerful outflowing winds shown by P Cyg structure at  $H\alpha$  and the Na I D lines; and by high Li I abundances (an indication of youth). All the known

FUors are located in star-forming regions. These characteristics defined the FU Ori class; their observed properties have been reviewed in detail by Herbig (1977) and by Hartmann & Kenyon (1996).

In recent years, some authors have chosen to take a broader and more inclusive view of the FUor phenomenon. For example, the list of Ábráham et al. (2004) contains some stars that are certainly not FUors in the original sense. We see no advantage in lumping such incompletely characterized objects in with those about which we know a great deal, such as FU Ori and V1057 Cyg. So we prefer to call them “FU Ori-like” (following Greene et al. 2008) until their status can be clarified. This paper deals with FU Ori.

One of best-documented FUors is V1057 Cyg, which before its flare-up by about 6 mag in 1971 was a faint variable star with an emission-line spectrum like that of a T Tauri star. After the flare-up, it appeared as a high-luminosity early-type star with only H $\alpha$  in emission. It has since been in slow decline, and is now (2008) only about 1 mag (in B) above its pre-outburst brightness.

FU Ori itself increased in brightness from  $m_{\text{pg}} = 16$  to 10 in 1937–1939, and since that time has remained near maximum, except for a slow decrease in optical brightness of about 0.15 mag per 10 years (Clarke et al. 2005). Before the flare-up, FU Ori was an irregular variable of unknown spectral type. Optically, it is now classified as G0, about luminosity class Ib. The spectral energy distribution shows an IR excess, typical for a pre-main-sequence star with circumstellar disk and/or dust shell. There is also excess flux in the UV region ( $\lambda < 2600 \text{ \AA}$ ) indicating the presence of a hot continuum of  $T_{\text{eff}} \approx 9000 \text{ K}$  (Kravtsova et al. 2007).

FU Ori has a faint red companion, probably a pre-main-sequence star, at a projected separation of  $0''.5 = 250 \text{ AU}$  (Wang et al. 2004). It is unknown whether the presence of this star has a connection to the outbursts.

A widely known concept is that FUors are solar mass pre-main-sequence stars that have increased dramatically in brightness due to a sudden episode of enhanced accretion triggered by some kind of disk instability. The rate of accretion has been estimated as  $2 \times 10^{-4} M_{\odot} \text{ yr}^{-1}$  by Popham et al. (1996, hereafter PKHN96) by fitting an accretion disk model to the observed spectral energy distribution. That is three orders of magnitude larger than in a classical T Tauri star. The optical spectra of FUors contain broad metallic lines that, according to Kenyon et al. (1988, hereafter KHH88), originate in the atmosphere of the inner accretion disk at radii of 8–80  $R_{\odot}$ .

There is general agreement that the IR excess seen in the SED of FU Ori originates in an extended envelope—presumably a disk—whose outline is seen in the  $K$ -band interferometric image of Malbet et al. (2005). In the model of Hartmann & Kenyon, this structure extends inward to the central star and overwhelms it: “during outburst, the disk outshines the central star by factors of 100–1000” (Hartmann & Kenyon 1996). Thus the optical spectrum of FU Ori is thought to be formed in an atmosphere atop the surface of this optically thick disk, and the contribution of the central star is small or negligible.

Because of the plausibility of this hypothesis, and the many subsequent papers that built upon it, it largely escaped the critical scrutiny that usually follows upon such an interesting new proposal. A simple yet critical test of the self-luminous accretion disk model can be provided by the higher-resolution optical spectra that have now become available. These make it possible to approach the key question: whether the *optical* line profiles are in fact those of a Keplerian disk or not.

One of the most explicit predictions of that FUor disk model is that line width (or  $v \sin i$ ) should depend on wavelength and excitation potential, because the warm central regions of the disk rotate faster than the cooler regions farther out. Observational evidence for such relationships in the optical spectra of FU Ori and V1057 Cyg were reported by Welty et al. (1992), but not confirmed later by spectroscopic data of higher quality and resolution (Herbig et al. 2003, hereafter HPD03). This paper deals with that issue in more detail.

Another prediction of the model was that FUor absorption lines should appear double because of Keplerian splitting. No such splitting is observed in the high-resolution spectra of FU Ori described in this paper. In V1057 Cyg, some (but not all) absorption lines appeared to be double, but as the star faded, it became clear that the duplicity was caused by the emergence of emission cores in the line centers that are produced in a hot region (which was called a “chromosphere” by HPD03 for lack of a better word).

## 2. Observations

This paper reports an analysis of absorption line profiles of FU Ori on new spectra obtained between 2003 and 2006 with the HIRES spectrograph on the Keck I telescope on Mauna Kea.<sup>1</sup> The dates of those observations are given in Table 1. The 2003 spectrograms covered the region 4350–6750 Å, while the remaining four covered 4750–8690 Å, both with interorder gaps. The nominal resolution was 48,000. The slit width projected on the sky was  $0''.86 \times 7''$ . The spectra were reduced by conventional IRAF procedures. The velocity zero-point of each exposure was checked by measures of atmospheric lines.

## 3. Photospheric Line Profiles

The new spectra of FU Ori appear similar to those of 1995–2000, described in detail by HPD03, and to the single observation of 1987 discussed by Petrov & Herbig (1992).  $H\alpha$  has a P Cyg profile with a strong blueshifted absorption extending to about  $-400 \text{ km s}^{-1}$  that is produced by an

---

<sup>1</sup>The W. M. Keck Observatory is operated as a scientific partnership among the California Institute of Technology, the University of California, and the National Aeronautics and Space Administration. The Observatory was made possible by the generous financial support of the W. M. Keck Foundation.

outflowing wind. A weaker longward emission component is also present. Both absorption and emission components vary from night to night. The wind absorption is always strong, while the emission component may disappear completely on some occasions (see D’Angelo et al. 2000 and Figs. 26 and 32 in HPD03).

On account of the high resolution and quality of the HIRES spectra, the distinctive profiles of photospheric lines are quite apparent. A sample of both strong and weak metallic lines is shown in Figure 1. The weaker lines have symmetric wings, while the stronger have either wider shortward wings (e.g., Ca I 6439) or a deep blueshifted absorption component (e.g., Mg I 5183, Fe II 5018). The stronger lines are formed in outer layers of the atmosphere; such profiles were described by Calvet et al. (1993) in terms of a disk wind model.

The weaker lines have a “boxy” shape, with steep wings and flat bottoms (Fig. 1, right panel). Fine structure can be seen at their bottoms, and sometimes narrow minima appear at one or both edges. Such profiles persist on a timescale of months and years. Figure 2 shows a sequence of six spectra of the 7530–7590 Å region, which contains a few outstanding metal lines. A spectrum of  $\beta$  Aqr (G0 Ib) taken with the same instrument is shown for comparison. In FU Ori, a slight profile asymmetry that changes from one spectrum to another is present: either the shortward or longward side of the profile becomes deeper. This variable asymmetry of photospheric lines was noticed earlier in the SOFIN spectra of FU Ori (HPD03), where a period of 3.5 days was suspected. The time spacing of the present HIRES observations is so large that although variations can be detected, the periodicity cannot be verified.

Here we concentrate on the profiles of weak photospheric lines, which are not affected by wind/shell absorptions and thus may carry information about the structure of photospheric layers. The equivalent widths (EW) of Fe I and other photospheric lines in FU Ori are about the same as in a G-type supergiant, but due to their large widths, those lines are very shallow. The weakest lines that we could measure on the HIRES spectra have EWs of approximately 0.05 Å and central depths of about 0.015 of the continuum.

In most previous spectroscopic studies of FUors, cross-correlation was used to improve the signal-to-noise ratio and to derive an “average” line profile over a certain spectral interval, while in these HIRES spectra we are able to measure the profile of each line individually.

Because of the large line widths, blending is a severe problem especially in the blue, so minimally blended lines were selected. Furthermore, some lines are accompanied shortward by wind (or shell) components, so only the longward half of those profiles could safely be considered to be purely atmospheric. Table 2 is a list of 59 lines selected as adequately free of blends or wind structure. The symbol  $r$  in the last column means that only the longward half of that profile is blend-free. The line parameters in Table 2 are taken from the Vienna Atomic Line Database (Kupka et al. 1999).

As a line width parameter, we selected the half-width at half-depth (HWHD) of the longward side of the profile, as illustrated in Figure 3. The standard deviation of one line measurement

is 1.5–2.0 km s<sup>-1</sup>. The value of HWHD, averaged over all the lines of Table 2, is given for each observation in Table 1, where  $\sigma$  in the fourth column is the standard deviation of the average in km s<sup>-1</sup>. The average HWHD is not the same on all six dates. The overall average is  $61.88 \pm 0.19$  km s<sup>-1</sup>, so the variations of HWHD, if real, do not exceed the  $\sigma$  in the fourth column of Table 1. Since HWHD is determined from the red wing only, any change in the radial velocity of FU Ori would cause a change in HWHD as well. Therefore, the constancy of HWHD within  $\pm 0.19$  km s<sup>-1</sup> is compatible with constancy of the radial velocity of FU Ori at that level.

Radial velocity shifts can also be obtained by cross-correlating each of the six spectra of FU Ori with their average. This procedure was done for the spectral intervals: 5995–6030, 6570–6620, and 7705–7765 Å; the results are listed as  $\Delta RV$  in Table 1. These radial velocity shifts between spectra do not exceed  $\pm 0.6$  km s<sup>-1</sup>; the standard deviation is 0.33 km s<sup>-1</sup>. The accuracy of this method is lower than that described above because slight changes in profile asymmetry may partly contribute to the apparent velocity shifts (HPD03). It is safe to conclude that the radial velocity of FU Ori derived from these six HIRES spectra was constant within  $\pm 0.3$  km s<sup>-1</sup> over this time interval.

#### 4. Comparison to Models

These new HIRES spectra of FU Ori make it possible to compare observations with the spectra predicted by accretion disk theory. In this section we first test whether line width depends on wavelength and excitation potential (EP). Then we compare the observed line *profiles* to those calculated for two different models: (1) a differentially rotating Keplerian disk, and (2) a rigidly rotating spherical star with a dark polar spot.

##### 4.1. Disk Model

The first models for FU Ori and V1057 Cyg, by KHH88, were thin accretion disks with temperature  $T_{\text{eff}}$  decreasing with distance  $r$  from the disk center as  $T_{\text{eff}} \propto r^{-3/4}$  and Keplerian rotational velocity  $v_{\text{rot}} \propto r^{-1/2}$ . In PKHN96, the model was improved by including a self-consistent treatment of the boundary layer region.

During the 20 years between the middle of 1980s, when the accretion disk model (KHH88) was put forward, and the beginning of our present HIRES observations in 2003, the brightness of FU Ori has dropped by only about 0.3 mag in  $B$ ,  $V$ , and  $R$  (Clarke et al. 2005), so we assume that the distribution of energy in the optical region did not change significantly, and so we begin by comparing the KHH88 model with our observations. That model predicts a specific dependence of line width on wavelength and excitation potential (EP), a prediction that has in many subsequent

papers on FUors been cited as observational support for the theory.

According to the KHH88 prescription, the disk can be considered as a sum of annuli, each of radius  $r$ , temperature  $T_{\text{eff}}(r)$ , and projected rotational velocity  $v \sin i$ , also a function of  $r$ ;  $i$  is inclination of the disk rotational axis to the line of sight. We use the same parameters of the model as in KHH88: radius of the central star  $5.5 R_{\odot}$ , inner radius of the disk  $r_{\text{in}} = 1.46 R_{*}$ , peak temperature  $T = 7200$  K at  $r_{\text{in}}$ ,  $v \sin i = 93 \text{ km s}^{-1}$  at  $r = 1 R_{*}$ ;  $v \sin i$  is the main parameter that determines spectral line width.

The intensity spectrum of each annulus can be represented by a synthetic spectrum emerging from the stellar atmosphere at a certain angle  $\theta$  between the line of sight and normal to the stellar surface. These synthetic spectra were calculated using the code by Berdyugina (1991) and Kurucz’s stellar atmosphere models (Kurucz 1993). We chose  $\theta = 45^{\circ}$  to make the spectra more appropriate for modeling an inclined disk. However, this parameter is not critical for line profiles in the integrated spectrum of the disk, as long as  $\theta < 60^{\circ}$ . The synthetic spectra were convolved with the rotational function (defined in KHH88) of the corresponding annulus in the disk, and convolved with a Gaussian profile corresponding to the spectral resolution of HIRES.

In the inner 18 annuli, within  $r = 6 R_{*}$ , the temperature decreases gradually from 7200 to 3500 K. Within this range, the following discrete set of  $T_{\text{eff}}$  was used for calculation of the synthetic spectra: 7200, 6500, 5750, 5000, 4500, 3750, 3500 K, with  $\log g = 2$ , and  $v_{\text{micro}} = 2 \text{ km s}^{-1}$ . This is about the same as the set of spectral templates from F2 to M1 types used in KHH88. Rotational velocity was calculated explicitly for each annulus as a function of its radius. For the outer 5–8 annuli with  $T_{\text{eff}} < 3500$  K ( $r = 6\text{--}13 R_{*}$ ), high-resolution spectra of late-type stars were obtained from the ESO/UVES spectral library: HD 95950 (M2 Ib) and HD 34055 (M6 V).

The contribution from each annulus to the integrated spectrum (as defined by its temperature and surface area) was taken from the KHH88 model. Spectra from each annulus with its contribution factor were added up to produce the integrated spectrum of the disk. The outer annuli with  $T_{\text{eff}} < 3500$  K contribute only a few percent to the optical spectrum of the disk. Moreover, the atomic lines discussed in this paper are formed within the inner regions of the disk, which are represented by the Kurucz model spectra. Nevertheless, we attempt to exclude from the analysis those atomic lines that fall near the strongest breaks in the continuum caused by molecular bands in the M-type spectra, which might distort the local continuum level in the integrated spectrum.

The only difference between this procedure and that described in KHH88 is that we used synthetic spectra of stellar atmospheres, while in KHH88 observed spectra of template stars were used. This may be important when fine structure of photospheric lines is considered. First, we examine whether line width is a function of EP and wavelength in both observed and calculated spectra.

Table 3 is a list of lines measured in the disk model spectrum. It is shorter than that in Table 2 because of more severe blending in the predicted spectrum of the disk. The error in the measurement of HWHM for one line is about the same ( $\pm 2.0 \text{ km s}^{-1}$ ) as in HIRES spectra. Although model

spectra are noiseless, there is always some uncertainty in locating the local continuum level. Figure 4 shows line width vs. EP and vs. wavelength for the HIRES spectrum of highest quality (2004 November 21) as filled circles, and for the model spectrum of the disk as open circles. HWHD vs. EP (filled circles in the left panel) show a correlation coefficient (CC) of 0.18, which with 59 data points corresponds to a false alarm probability (FAP) of 20%; i.e., there is no correlation of HWHD with EP. In any case, the line slope is opposite to that expected from the disk model.

On the right panel, HWHD vs. wavelength, the filled circles show a weak correlation (CC = 0.34) in the sense of line width increasing toward longer wavelength, but again, that is in the opposite sense to that predicted by the disk model. As expected, the disk model (open circles) predicts a clear dependence of line width on wavelength. (The larger scatter of points in the model plot is caused by the dependence of line width on both of these parameters.)

So, in contrast to the model prediction, the observed HWHDs in FU Ori show no dependence on either EP or wavelength. This result was checked for each of the six spectra of FU Ori (see Fig. 5). It confirms the conclusion of our previous paper (HPD03), but the higher quality of the new Keck spectra makes the result more firm.

The disk model also predicts a doubling of photospheric absorption lines, which is not evident in these spectra of FU Ori, where the line profiles have rather flat bottoms. Nevertheless, when the HIRES spectra of FU Ori are cross-correlated with the spectrum of a G0 Ib template ( $\beta$  Aqr), the cross-correlation function is slightly doubled, similar to that seen in the earlier observations of 1995–2000 (HPD03), and in the single spectrogram of 1987 (Petrov & Herbig 1992). This is due to the narrow absorption dips flanking the flat bottom of the line profile; this effect is discussed in an alternative model below. Line doubling may be also caused by the presence of emission cores in the line centers, an effect that actually was observed in V1057 Cyg after 1995, when that star dropped in brightness and some emission cores rose above the continuum level (Petrov et al. 1998). Such an emission core in Li I  $\lambda$ 6707 may be present in some of our spectra of FU Ori.

In our discussion (Petrov & Herbig 1992) of a spectrogram of FU Ori obtained in 1987 January (at a resolution comparable to HIRES), we noted that although not striking, a doubling of metallic lines was detectable at that time by cross-correlation against a standard supergiant. In the case of the HIRES spectra discussed here, although variable structure is apparent, no duplicity is evident on cross-correlation. The earlier SOFIN spectra showed that the line profiles change from night to night (Fig. 29 in HPD03), so there is no evidence of a secular change in the line structure.

The new HIRES spectra were also compared to those predicted by the boundary layer model of PKHN96. In that model for FU Ori, the boundary layer is an annulus extending from the stellar surface to about  $2.2 R_*$ . The expected rotational profile differs from the Keplerian in such a way that maximum rotational velocity of  $47 \text{ km s}^{-1}$  is at  $2.2 R_*$ , while closer to the stellar surface the rotation decreases to  $33 \text{ km s}^{-1}$ . Within the boundary layer, the temperature ranges from 8200 to 5400 K. Outside the boundary layer the disk parameters approach those of the classical Keplerian thin disk. Thus, the optical spectrum is formed mostly within the boundary layer, and all spectral

lines with EP from 2 to 8 eV have about the same width. Only lines of 0–1 eV, formed in the distant regions of the disk, are a few  $\text{km s}^{-1}$  narrower. The dependence of line width on EP for the PKHN96 model is shown by the dashed line in Figure 4 (left). It is much lower than the observed curve because of the low rotational velocity in the boundary layer, as specified by PKHN96 for FU Ori. The line at  $6170 \text{ \AA}$  used by PKHN96 to fit their model to observations is not a good indicator of line width because it is a blend of three lines (Ca I 6169.04, 6169.56 and Fe I 6170.51) that are of comparable strength at  $T_{\text{eff}} = 5000\text{--}6000 \text{ K}$ . The blend cannot be resolved because the width of each component is  $\approx 2.5 \text{ \AA}$ , due to rotational broadening.

We conclude that the observed line widths of FU Ori do not follow the relations predicted by the Keplerian disk model. We remark also that the narrower widths of low excitation lines of the PKHN96 model would have been obvious on these HIRES spectra, if present.

Still more information can be retrieved from the FU Ori line profiles. In Figure 6 observed line profiles are compared with those of the Keplerian accretion disk model. The main differences between observed and modeled profiles—dependence of the model line width on EP, and the line doubling—can be seen even in this small spectral region. When the PKHN96 model is used, the match is worse, because those modeled lines are narrower and deeper than observed and have more prominent doubled structure.

The wings of lines in FU Ori are steeper than in the classical case of a rotating spherical star having reasonable limb darkening. The Keplerian disk also produces a rather smooth profile. A ring or torus (like the boundary layer) might produce lines with steep wings, but it would also produce a prominent hump in the line center. The flat bottom and steep wings that are actually observed are typical of another kind of object: a fast-rotating star with dark polar spot. Therefore we now examine a simple “star-spot” model (as was first applied to FU Ori by Herbig 1989).

## 4.2. “Star-spot” Model

A dark spot on the surface of a rotating star produces a bump in the otherwise smooth rotationally broadened profile of an absorption line. As the star rotates, the spot passes across the visible hemisphere, and the bump travels across the line profile. This effect is utilized in the Doppler imaging technique. If a large dark spot is located at the pole of rotation, line profiles remain disturbed throughout the period. Figure 7 shows a star with a polar spot and illustrates the consequence: a flat bottom in the line profile. Figure 8 shows how the line profile (of Ni I  $7555.59 \text{ \AA}$ , as an example) responds to different model parameters. (There are similar spots on both poles in this model, but only one is visible.) Only two free parameters are required to fit the model to the observed profiles: the inclination of the rotational axis ( $i$ ) and the spot radius ( $R_{\text{spot}}$ ). The value of  $v \sin i = 70 \text{ km s}^{-1}$  is fixed by the observed width of lines at continuum level.

An upper limit to the spot temperature can be set by the absence of TiO bands and other M-type features in the optical region (see Fig. 9). If the spot were hotter, the TiO band would be

apparent in the stellar spectrum. With  $T_{\text{spot}} < 3300$  K, the ratio of spot to photosphere brightnesses  $B_{\text{spot}}/B_{\text{phot}}$  would be less than 0.17 in the red. With the spot area occupying 30% of the visible hemisphere in projection, the contribution of the spot to the total spectrum would be less than 5%.

The model spectrum of the spotted star was calculated using the synthetic intensity spectrum with  $T_{\text{eff}} = 5000$  K,  $\log g = 2$ ,  $v_{\text{micro}} = 2$  km s<sup>-1</sup> for the photosphere, and  $T_{\text{eff}} = 3500$  K for the spot. Those spectra were convolved with the instrumental profile and integrated over the corresponding areas of the visible stellar hemisphere, with the limb darkening coefficient 0.7, inclination  $i$ , and  $v = 70/\sin i$  km s<sup>-1</sup>.

In Figure 10 the observed line profiles are compared to those of the “star-spot” model that results from this calculation. The best match was achieved with  $R_{\text{spot}} = 40^\circ$  and  $i = 37^\circ$  (there is freedom of a few degrees in the choice of those parameters). Such a spot occupies 12% of the global stellar surface (about 30% in projection on the visible stellar hemisphere). Note the narrow absorption dips at both sides of the flat bottom, which appear at a certain inclination and spot radius. These features make the profile appear slightly doubled: cross-correlation of the “star-spot” model spectra with the template G0 spectrum also shows that double structure.

Clearly, the “star-spot” model fits the observations of FU Ori much better than either disk model. Note that in making this fit, we consider relatively weak photospheric lines of metals having  $\text{EW} \approx 0.1$  Å. The structure of stronger lines often includes shortward-shifted absorption features formed in the expanding shell and, in some cases, emission cores. Figure 11 shows the observed spectrum of FU Ori around the Li I  $\lambda 6707$  line on two occasions: the Li line is strong due to the enhanced Li abundance in FU Ori; the same section calculated with the “star-spot” model is shown for comparison. The two spectra of FU Ori differ in the shortward wing: the deep absorption at  $-40$  km s<sup>-1</sup> is prominent on 2005 November 23 (it is also present at lesser strength in other spectra of FU Ori) and, when present, causes the line to appear double. Comparison to the “star-spot” model shows that any emission core, if present, is very weak. Such shortward-shifted shell lines tend to be stronger in the blue region.

## 5. Summary

There is no doubt that FU Ori possesses a disk: radiation from the disk and envelope dominates the IR, the outline of the disk was resolved at AU scale by IR interferometry (Malbet et al. 2005), and the distribution of energy in the infrared is compatible with a disk model. So our question was: what is it that is seen in the optical region, a central star or an inner accretion disk?

We found that (1) all weak photospheric lines have the same line width and profile, as expected for a rigidly rotating body, but in definite conflict with prediction for the self-luminous Keplerian disk model; (2) those profiles can be explained if the central object is a rapidly rotating high-luminosity star with a dark polar spot; and (3) there is no sign of the line doubling, or the dependence of line width on wavelength (in the optical region) that is expected for the disk model.

In any disk, the temperature and rotational velocity change with radius, and this defines the width of spectral lines in integrated light. It would be strange if the disk temperature and velocity profiles were designed by nature in such a way that all atomic lines formed in different parts of the disk were of equal width. It is more natural to assume that the optical spectrum of FU Ori is produced at the central object, while the IR spectrum is formed in the circumstellar disk (as in classical T Tauri stars), and the  $2.3\ \mu\text{m}$  CO lines—a characteristic feature of FUors—are formed in a cool disk or a distant shell. Certainly there is no evidence of TiO bands or other M-type features in the optical region: see Figure 9.

Do these results undermine the self-luminous accretion disk hypothesis in a significant way? No, but they do demonstrate that some modification is in order. It is remarkable that the hypothesis still stands even though two of the strongest observational arguments that were originally urged in its favor are now seen, in the case of the prototype, to be invalid.

P. P. acknowledges the support of grant INTAS 03-516311 during this investigation, and G. H. is indebted to the National Science Foundation, grant AST 02-04021 for partial support. We thank Ann Boesgaard, who obtained the two 2002 HIRES spectrograms of FU Ori at our request, and Suzan Edwards, Bo Reipurth, and Steve Stahler for helpful comments.

## REFERENCES

- Ábráham, P., Kóspál, Á., Csizmadia, Sz., Kun, M., Moór, A., & Prusti, T. 2004, *A&A*, 428, 89
- Berdyugina, S. V. 1991, *Bull. Crimean Astrophys. Obs.*, 83, 89
- Calvet, N., Hartmann, L., & Kenyon S. 1993, *ApJ*, 402, 623
- Clarke, C. J., Lodato, G., Melnikov, S. Y., & Ibrahimov, M. A. 2005, *MNRAS*, 361, 942
- D’Angelo, G., Errico, L., Gomez, M. T., Smaldone, L. A., Teodorani, M., & Vittone, A. A. 2000, *A&A*, 356, 888
- Greene, T. P., Aspin, C., & Reipurth, B. 2008, *AJ*, 135, 1421
- Hartmann, L., & Kenyon, S. J. 1996, *ARA&A*, 34, 207
- Herbig, G. H. 1977, *ApJ*, 217, 693
- Herbig, G. H. 1989, in *ESO Workshop on Low-Mass Star Formation and PMS Objects*, ed. B. Reipurth (Garching: ESO), 233
- Herbig, G. H., Petrov, P. P., & Duemmler, R. 2003, *ApJ*, 595, 384 (HPD03)
- Kenyon, S. J., Hartmann, L., & Hewett, R. 1988, *ApJ*, 325, 231 (KHH88)
- Kravtsova, A. S., Lamzin, S. A., Errico, L., & Vittone, A. 2007, *Astronomy Letters*, 33,755
- Kupka, F., Piskunov, N. E., Ryabchikova, T. A., Stempels, H. C., & Weiss, W.W. 1999, *A&AS*, 138, 119
- Kurucz, R. L. 1993, *ATLAS9 Stellar Atmosphere Programs and 2 km/s grid*. Kurucz CD-ROM No. 13 (Cambridge, MA: Smithsonian Astrophysical Observatory)
- Malbet, F., et al. 2005, *A&A*, 437, 627
- Petrov, P. P., & Herbig, G. H. 1992, *ApJ*, 392, 209
- Petrov P. P., Duemmler R., Ilyin I., & Tuominen I. 1998, *A&A*, 331, L53
- Popham, R., Kenyon, S., Hartmann, L., & Narayan, R. 1996, *ApJ*, 473, 422 (PKHN96)
- Wang, H., Apai, D., Henning, T., & Pascucci, I. 2004, *ApJ*, 601, L83
- Welty, A. D., Strom, S. E., Edwards, S., Kenyon, S. J., & Hartmann, L.W. 1992, *ApJ*, 397, 260

Table 1. HWHD, Averaged over the Lines Listed in Table 2, and  $\Delta RV$ , Radial Velocity Shifts by Cross-Correlation

Date	JD	HWHD ( $\text{km s}^{-1}$ )	$\sigma$ ( $\text{km s}^{-1}$ )	$\Delta RV$ ( $\text{km s}^{-1}$ )
2003 Jan 11	52650.85	61.77	0.29	0.56
2003 Feb 11	52681.81	61.64	0.27	0.10
2004 Sep 24	53273.09	61.96	0.29	0.31
2004 Nov 21	53331.05	61.77	0.24	-0.31
2005 Nov 23	53698.12	62.04	0.28	-0.53
2006 Dec 10	54079.97	62.16	0.23	0.29

Table 2. Lines Selected for Measurement of the HWHD at the Longward Wing

$\lambda$ (Å)	Ion	EP (eV)	Note <sup>a</sup>	$\lambda$ (Å)	Ion	EP (eV)	Note <sup>a</sup>
5383.37	Fe I	4.31	...	6726.66	Fe I	4.61	r
5717.83	Fe I	4.28	...	6767.79	Ni I	1.83	-
5772.15	Si I	5.08	...	6810.26	Fe I	4.61	-
5775.08	Fe I	4.22	...	6814.94	Co I	1.96	r
5862.35	Fe I	4.55	...	6828.59	Fe I	4.64	r
5899.29	Ti I	1.05	...	7090.38	Fe I	4.23	r
5922.11	Ti I	1.05	...	7122.19	Ni I	3.54	-
5934.66	Fe I	3.93	...	7344.70	Ti I	1.46	r
5965.83	Ti I	1.88	...	7393.60	Ni I	3.61	-
5987.07	Fe I	4.80	r	7445.75	Fe I	4.26	r
6016.66	Fe I	3.55	...	7511.02	Fe I	4.18	-
6024.06	Fe I	4.55	r	7525.11	Ni I	3.63	r
6027.05	Fe I	4.09	...	7555.60	Ni I	3.85	-
6056.01	Fe I	4.73	r	7568.89	Fe I	4.28	-
6108.11	Ni I	1.68	...	7574.04	Ni I	3.83	-
6180.20	Fe I	2.73	...	7586.01	Fe I	4.31	r
6270.23	Fe I	2.86	...	7727.61	Ni I	3.68	r
6355.03	Fe I	2.85	r	7780.55	Fe I	4.47	-
6358.70	Fe I	0.86	...	7788.94	Ni I	1.95	-
6380.74	Fe I	4.19	r	7855.44	Fe I	5.06	-
6411.65	Fe I	3.65	...	7912.87	Fe I	0.86	-
6439.08	Ca I	2.53	...	7937.13	Fe I	4.33	-
6471.66	Ca I	2.53	r	8075.15	Fe I	0.92	r
6475.62	Fe I	2.56	r	8080.55	Fe I	3.30	-
6569.22	Fe I	4.73	...	8085.18	Fe I	4.45	r
6581.21	Fe I	1.49	...	8426.51	Ti I	0.83	r
6586.31	Ni I	1.95	...	8611.80	Fe I	2.85	-
6707.89	Li I	0.00	...	8621.60	Fe I	2.95	-
6717.68	Ca I	2.71	r	8648.47	Si I	6.21	-
6721.85	Si I	5.86	...				

<sup>a</sup>r = only the longward half of that profile is blend-free.

Table 3. HWHD of Selected Lines in the Composite Spectrum of Accretion Disk

$\lambda$ ( $\text{\AA}$ )	Ion	EP (eV)	HWHD ( $\text{km s}^{-1}$ )	$\lambda$ ( $\text{\AA}$ )	Ion	EP (eV)	HWHD ( $\text{km s}^{-1}$ )
5965.83	Ti I	1.88	49.9	7525.11	Ni I	3.63	54.2
6016.66	Fe I	3.55	66.8	7555.59	Ni I	3.85	57.6
6024.06	Fe I	4.55	59.3	7568.89	Fe I	4.28	53.7
6027.05	Fe I	4.08	53.7	7574.04	Ni I	3.83	55.6
6039.72	V I	1.06	47.1	7586.01	Fe I	4.31	56.8
6358.69	Fe I	0.86	52.5	7714.31	Ni I	1.93	52.3
6371.37	Si II	8.12	74.8	7727.61	Ni I	3.68	58.5
6569.22	Fe I	4.73	60.0	7738.96	Ti I	1.46	41.9
6581.21	Fe I	1.49	47.4	7767.44	Ti I	0.90	40.0
6586.31	Ni I	1.95	54.7	7788.94	Ni I	1.95	49.8
6707.89	Li I	0.00	50.5	7912.87	Fe I	0.86	45.8
6717.68	Ca I	2.71	59.3	7937.13	Fe I	4.33	57.0
6721.85	Si I	5.86	69.3	8075.15	Fe I	0.92	47.9
6726.66	Fe I	4.61	57.5	8080.54	Fe I	3.30	50.3
6767.77	Ni I	1.83	57.2	8085.18	Fe I	4.45	57.3
6772.31	Ni I	3.66	61.4	8611.80	Fe I	2.85	48.6
6806.85	Fe I	2.73	52.2	8621.60	Fe I	2.95	51.8
6814.94	Co I	1.96	48.8	8648.46	Si I	6.21	59.5
7511.02	Fe I	4.18	57.1				

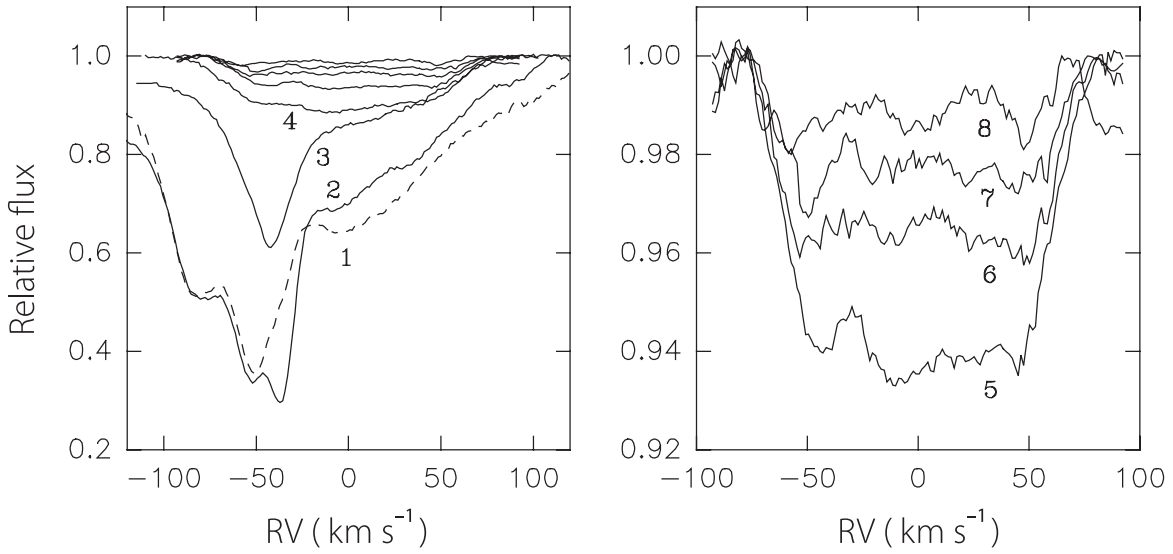


Fig. 1.— Line profiles in FU Ori. Left panel: (1) Mg I 5183.60, (2) Fe II 5018.44, (3) Fe II 5316.61, (4) Ca I 6439.08. Profiles of some weaker lines are expanded in the right panel: (5) Fe I 7511.02, (6) Ni I 7393.60, (7) Fe I 8080.55, (8) Fe I 7107.46. No smoothing or filtering was performed on these spectra. The S/N ratio at the continuum level in the 6000–7000 Å region is about 600.

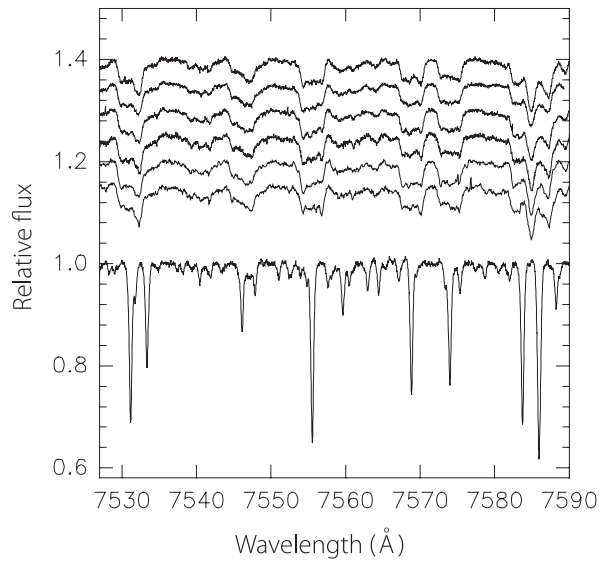


Fig. 2.— Fragments of FU Ori spectra of 2003–2006. The lower spectrum is of  $\beta$  Aqr (G0 Ib).

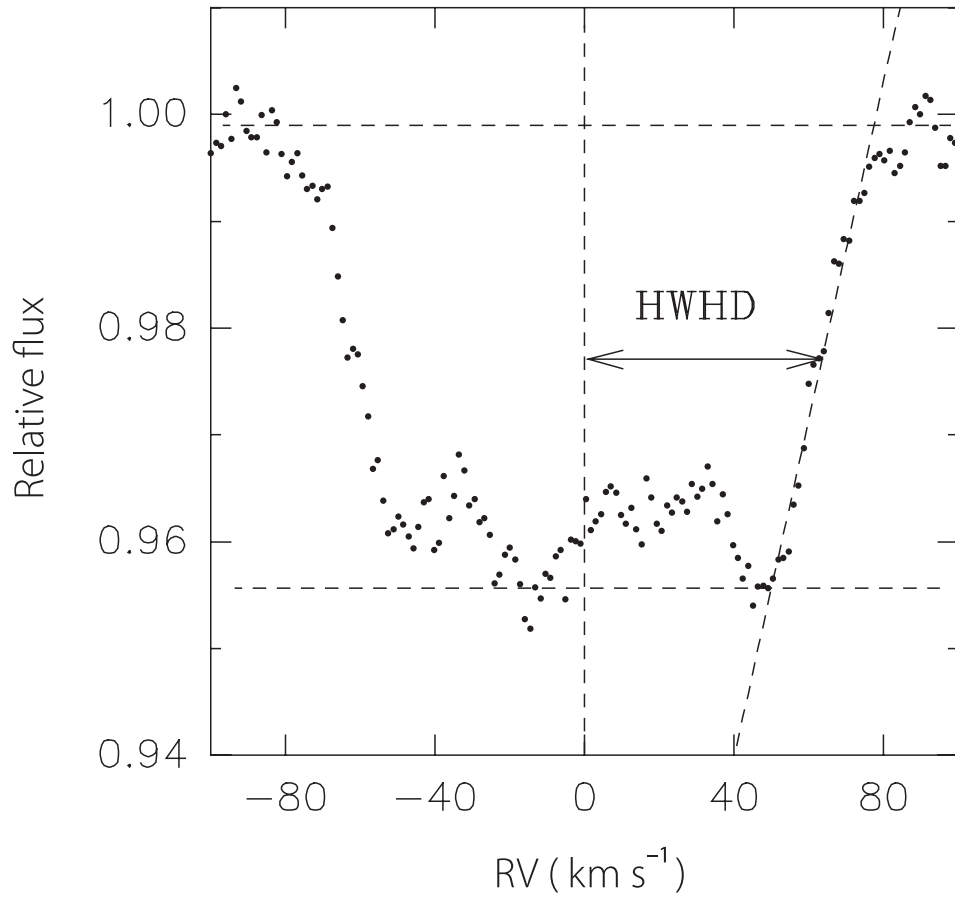


Fig. 3.— Line profile of Fe I 7568.89 and definition of the “half-width at half-depth” (HWHD).

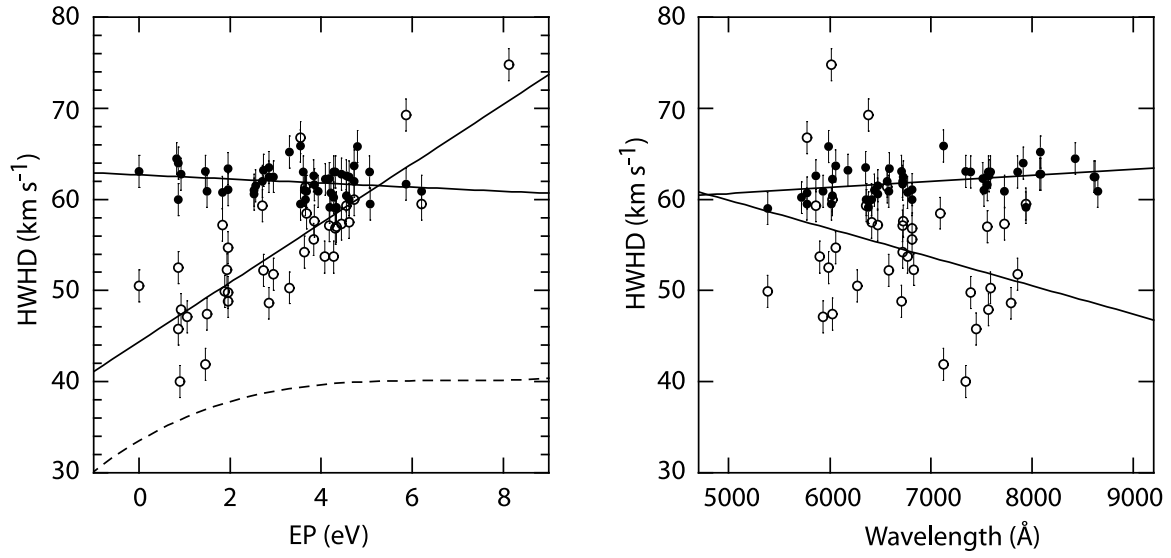


Fig. 4.— The dependence of line width (HWHD) on excitation potential (EP) is shown in the left panel, and its dependence on wavelength in the right. Filled circles indicate observed values, open circles those predicted by the model. The significance of the regression line slopes is discussed in the text. The data are from the spectrum of 2004 November 21.

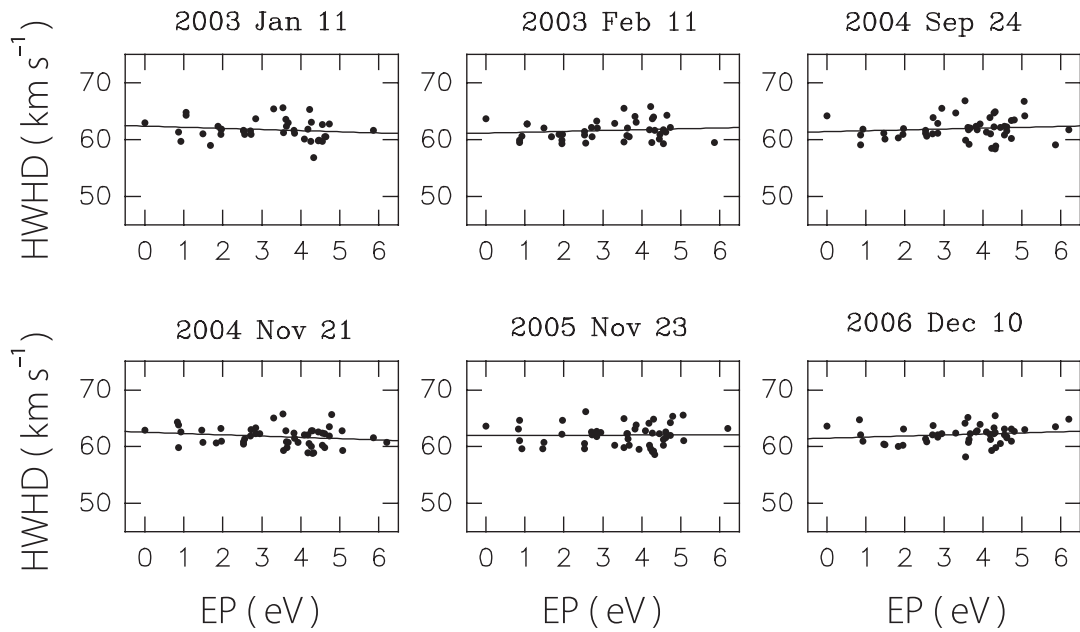


Fig. 5.— HWHD versus EP in each of the six HIRES spectra of FU Ori.

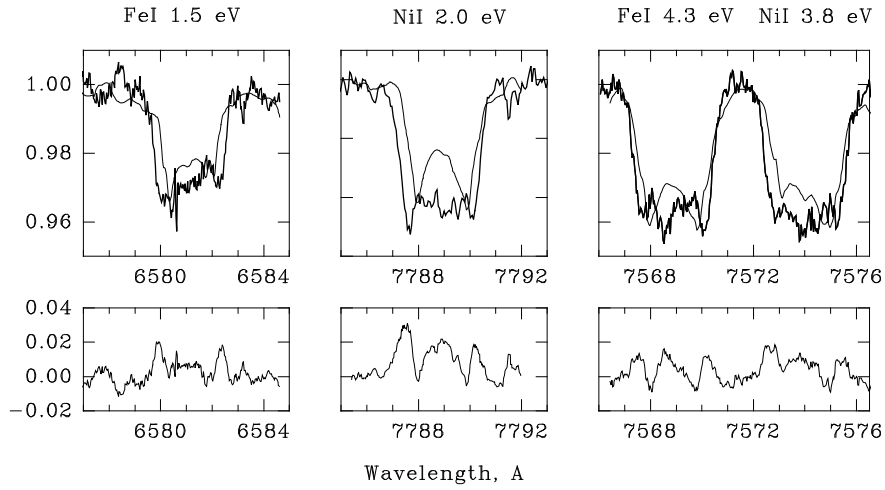


Fig. 6.— Comparison of observed line profiles (thick) to those calculated in the disk model (thin). Note that the width of the modeled profiles depends on EP. In the first and third panels, Fe I 6581.21, Fe I 7568.89 and Ni I 7574.04 were taken from the exposure of 2004 November 21; in the second panel, Ni I 7588.94 is from 2003 February 11. The bottom panels show the differences, model minus observed, in units of continuum intensity.

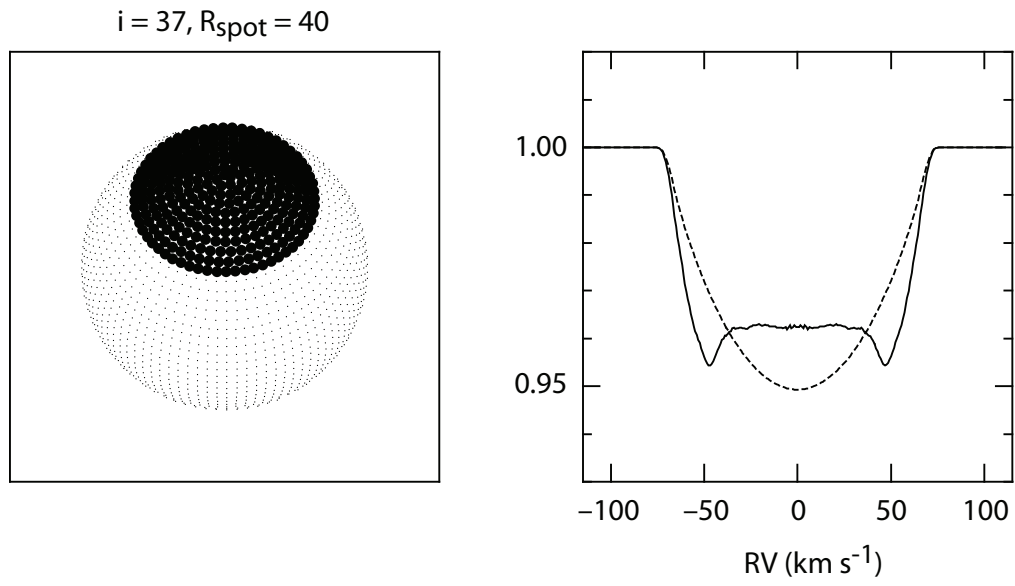


Fig. 7.— Left panel: model of a star with a dark polar spot. Right: typical line profile in the star with the polar spot (solid) as compared with unspotted star (dashed).

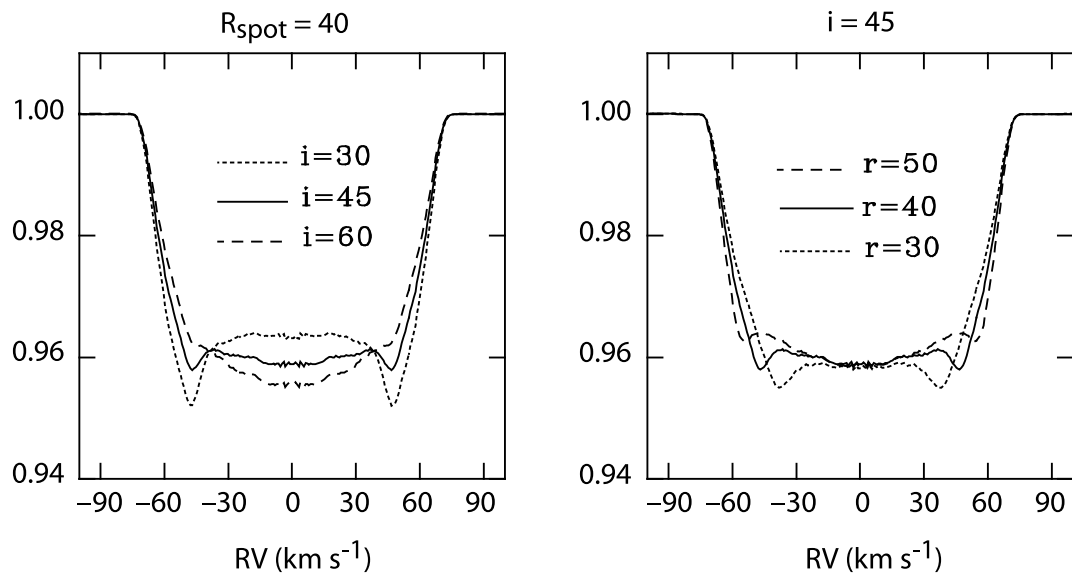


Fig. 8.— Line profiles in the “star-spot” model as a function of spot radius and inclination of the rotational axis to line of sight. Spot radius and inclination are in degrees.

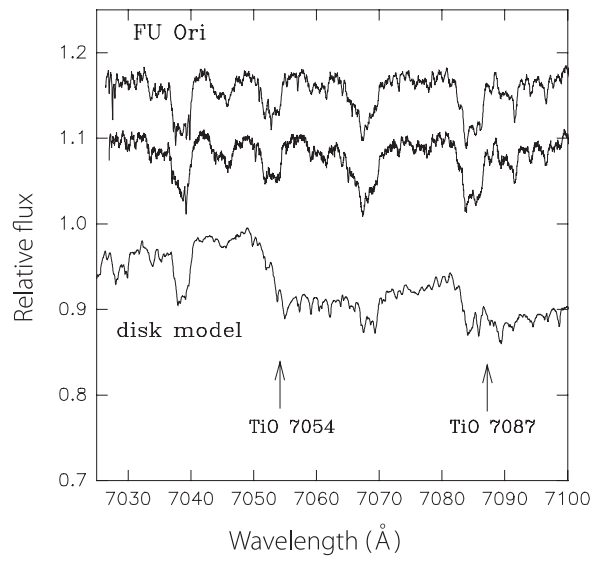


Fig. 9.— The region of the  $\lambda$  7054 TiO bands in observed spectra of FU Ori (upper: 2004 September 24, lower: 2006 December 10) and in the disk model.

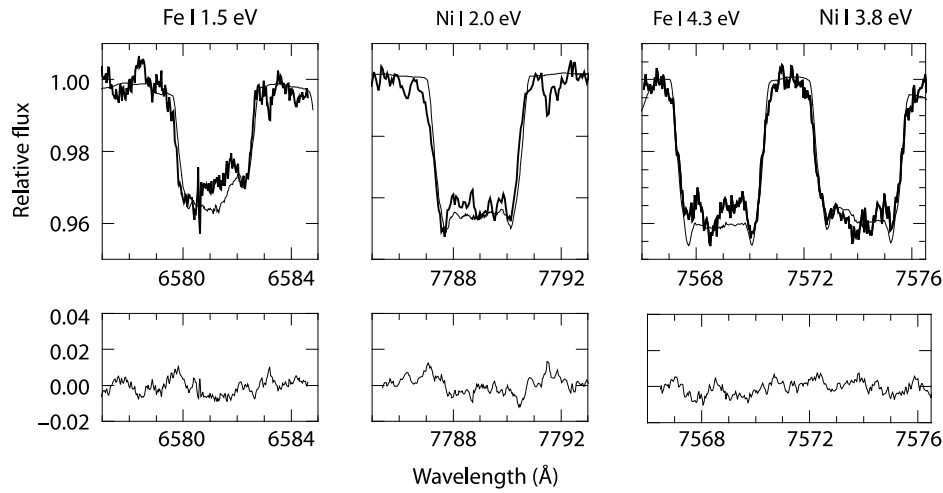


Fig. 10.— Comparison of observed line profiles (thick) to those calculated in the “star-spot” model (thin). The lines are the same as in Fig. 6. As in Fig. 6, the bottom panels show the differences, model minus observed, in units of continuum intensity.

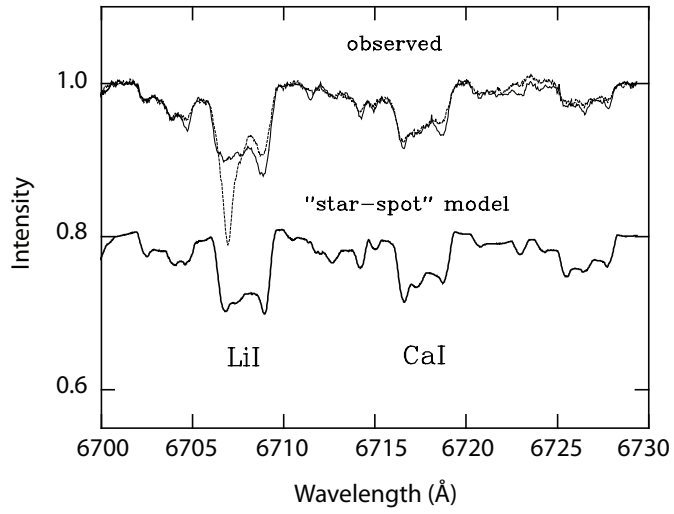


Fig. 11.— Top: the region of Li I  $\lambda$  6707 in FU Ori on 2003 January 11 (heavy solid line) and on 2005 November 23 (light line). Bottom: the same region from the “star-spot” model.